Dalton Transactions

Accepted Manuscript

ROYAL SOCIETY OF CHEMISTRY

www.rsc.org/dalton

Graphical Abstarct.

Novel heterometallic iodides $[\{(en)_2(PbAgI_3)\}]_{2n}\cdot nH_2O$ (**1**), $[(pda)_2(PbAgI_3)]_n$ (**2**), $[(tmeda)(PbAgI_3)]_n$ (**3**), $[(trien)(PbAgI_3)]_n$ (**4**), $[(tepa)(PbAg_2I_4)]_n$ (**5**), $[\{(dien)_3(CO_3)\}_2(Pb_6Ag_8I_{15})]_nI_n$ (**6**) were prepared by the reactions of PbI_2, AgI (or Ag_2CO_3) and KI with different polyamines in DMF solution. **1**–**6** represent a new type of hybrid organic-inorganic heterometallic iodides containing coordinative organic components.

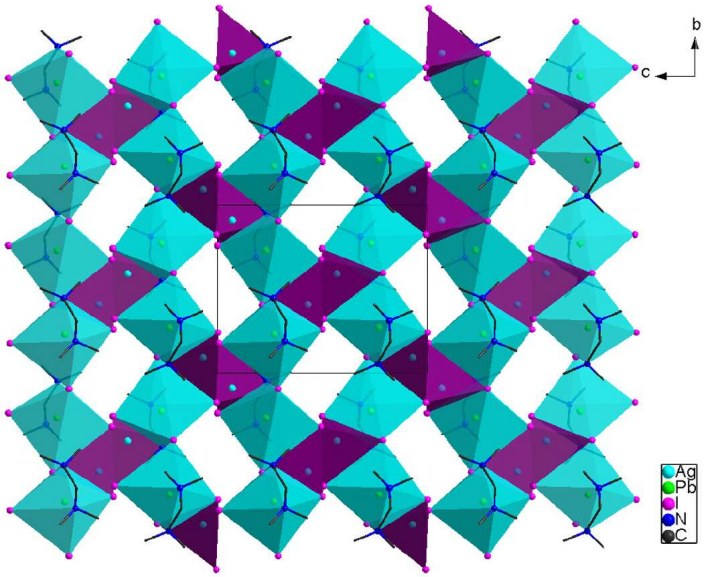

Syntheses and properties of 2-D and 3-D Pb–Ag heterometallic iodides decorated by ethylene polyamines at Pb(II) center

Yali Shen, Jialin Lu, Chunying Tang, Wang Fang, Dingxian Jia*, and Yong Zhang

Received (in XXX, XXX) Xth XXXXXXXXX 200X, Accepted Xth XXXXXXXXX 200X
First published on the web Xth XXXXXXXXX 200X
DOI: 10.1039/b000000x

Hybrid organic-inorganic Pb-Ag heterometallic iodides $[(en)_2(PbAgI_3)]_{2n}\cdot nH_2O$ (**1**), $[(pda)_2(PbAgI_3)]_n$ (**2**), $[(tmeda)(PbAgI_3)]_n$ (**3**), $[(trien)(PbAgI_3)]_n$ (**4**), $[(tepa)(PbAg_2I_4)]_n$ (**5**), and $[\{(dien)_3(CO_3)\}_2(Pb_6Ag_8I_{15})]_nI_n$ (**6**) were prepared by the reactions of PbI_2, AgI (or Ag_2CO_3) and KI with different polyamines in N,N′-dimethylformamide (DMF) solution. In **1**–**4**, two AgI_4 tetrahedra share a common edge to form the bimeric Ag_2I_6 unit. It coordinates to the Pb(II) ion of $[PbL_2]^{2+}$ or $[PbL']^{2+}$ (L = en, pda; L′ = tmeda, trien) via iodine atoms to form hybrid organic-inorganic heterometallic iodides **1**, **2**, **3** and **4**, respectively. Compounds **1**, **3**, **4** contain 2-D layered backbones of $[PbAgI_3]_n$, whereas, **2** contains a backbone $[PbAgI_3]_n$ with 3-D structure. Steric hindrance and denticity of the ethylene polyamines influence the coordination modes and connection strength between the iodoargentate aggregates and Pb(II) ions. In **5**, the AgI_4 units are joined via sharing common edges to form 1-D polymeric $[Ag_2I_4]_n^{2n-}$ anion. It is connected with $[Pb(tepa)]^{2+}$ via iodine atoms to form a 3-D network of $[(tepa)(PbAg_2I_4)]_n$. In **6**, the CO_3^{2-} ion binds three $[Pb(dien)]^{2+}$ units to form the novel trinuclear $[\{Pb(dien)\}_3(\mu_3\text{-}CO_3)]^{4+}$ complex ion. Eight AgI_4 tetrahedra are connected via sharing common edges to give a novel Ag_8I_{15} cluster with C_3 symmetry. The Ag_8I_{15} cluster and $[\{Pb(dien)\}_3(CO_3)]^{4+}$ unit are connected into a novel layered heterometallic iodometallate cation $[\{(dien)_3(CO_3)\}_2(Pb_6Ag_8I_{15})]_n^{n+}$ via sharing iodine atoms. Compounds **1**–**6** represent a new type of hybrid organic-inorganic heterometallic iodides containing coordinative organic components. Optical absorption spectra show blue shift of the absorption edges for **1**–**6** compared with those of the bulk PbI_2 and AgI solids.

Introduction

Hybrid organic-inorganic compounds are continuously of high interest due to the opportunity to combine useful properties of both components, and the possibility to tune the physical properties by the organic components.[1] Being one of important fields of the hybrid organic-inorganic materials, organic hybrid halometallates, such as haloplumbates and haloargentates, have attracted increasing interest because of their wide range of structural topologies and interesting physical properties, in particular optical and semiconducting properties, and phase transitions.[2,3] The structures of haloplumbates and haloargentates are characterized by the condensation of PbX_6 and AgX_4 (X = Cl, Br, I) primary units via corner-, edge-, or face-sharing in presence of cations as structure-directing agents. A large number of organoammonium haloplumbate and haloargentate salts have been prepared using ammonium cations as the structure-directing agents.[4,5] The organoammonium cations act as counterions to the inorganic component in the final halometallates. The examples of iodoplumbate and iodoargentate salts include discreted clusters $[Pb_{18}I_{44}]^{8-}$,[4a] $[Pb_3I_{10}]^{4-}$, $[Pb_7I_{22}]^{8-}$, $[Pb_{10}I_{28}]^{8-}$,[4b] $[Pb_5I_{16}]^{6-}$,[4c] and $[Ag_4I_8]^{4-}$,[5a] one-dimensional chains $[PbI_5]^{3-}$,[3a, 3d] $[PbI_3]^-$, $[Pb_2I_6]^{2-}$, $[Pb_{10}I_{24}]^{4-}$,[4d-f] $[Pb_3I_{14}]^{8-}$, $[Pb_5I_{22}]^{12-}$,[4g] $[Ag_2I_4]^{2-}$,[5b, 5c] $[Ag_4I_6]^{2-}$,[5d] and $[Ag_5I_7]^{2-}$,[5e] two-dimensional layers $[PbI_4]^{2-}$,[3c, 4h, 4i] $[Pb_3I_9]^{3-}$,[4j] $[Pb_7I_{18}]^{4-}$,[4b] $[Pb_2I_7]^{3-}$, $[Pb_5I_{14}]^{4-}$,[4k] $[Pb_4I_{18}]^{10-}$,[4l] and three-dimensional framework $[Pb_7I_{18}]^{4-}$.[4m] The stoichiometry and dimensionality, and the metal-iodide linkages of these iodometallates are extremely sensitive to specific reaction conditions, and the nature of the cations with both size and functionality playing a crucial role.[3c,4b,4g] Recently, transition-metal (TM) and lanthanide (Ln) complex cations have been used as structure-directing agents, and several TM- or Ln-containing iodoplumbates and iodoargentates have been prepared in the co-presence of TM^{2+} (or Ln^{3+}) ions and coordinative organic molecules.[6–9] In addition, some silver iodide adducts with organic ligands have been reported.[10]

Recently, the heterometallic iodometallates, which are constructed by mixed octahedral MI_6 (such as PbI_6 and BiI_6) and tetrahedral MI_4 (such as CuI_4, AgI_4, HgI_4) units are attracting much interest in view of the structural diversity and unusual optical and electrical properties embedded in combination of the two type structural units. However, only a few examples of heterometallic iodobismuthates and iodoplumbates have been reported sofar.[11, 12] Now, the PbI_2/AgI/KI system is investigated in coordinative polyamines (Scheme 1), and hybrid organic-inorganic Pb-Ag heterometallic iodides $[\{(en)_2(PbAgI_3)\}]_{2n}\cdot nH_2O$ (**1**), $[(pda)_2(PbAgI_3)]_n$ (**2**), $[(tmeda)(PbAgI_3)]_n$ (**3**), $[(trien)(PbAgI_3)]_n$ (**4**), $[(tepa)(PbAg_2I_4)]_n$ (**5**), $[\{(dien)_3(CO_3)\}_2(Pb_6Ag_8I_{15})]_nI_n$ (**6**) were synthesized. **1**–**6** represent a new type of hybrid organic-inorganic heterometallic Pb–Ag iodometallates. They are different from compounds $[(Bu_4N)(PbAgI_4)]_n$[11b] and $[Ln(DMSO)_8]_2Pb_3Ag_{10}I_{22}$,[12] in which

the heterometallic iodometallate anions are formed by copolymerization of PbI_6 octahedron and AgI_4 tetrahedron. They are also different from the above organoammonium iodoplumbate and iodoargentates, in which the organic components just act as counterions to the iodometallate anions. Compounds **1**–**6** consist of $[PbAgI_3]_n$ (**1**–**4**), $[PbAg_2I_4]_n$ (**5**) or $[(\mu_3\text{-}CO_3)_2(Pb_6Ag_8I_{15})]_n$ (**6**) backbones constructed by AgI_4 tetrahedra and Pb(II) ions. The organic components bind the backbones at the Pb(II) centers via Pb–N bonds to satisfy coordination site of the Pb(II) ions. Herein, we report on the preparation, X-ray structural characterization, optical absorption spectra and thermal stabilities of the Pb–Ag heterometallic iodides containing coordinated polyamines.

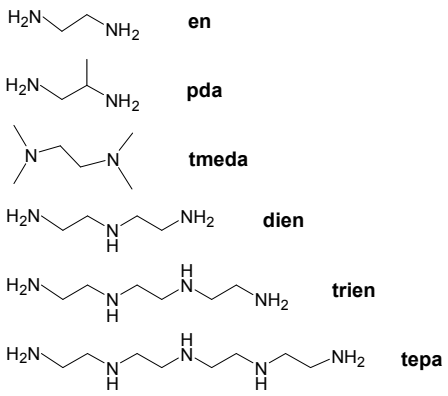

Scheme 1.

Experimental

Materials and General Methods

All materials were of analytical grade and were used as received. Elemental analyses were performed using an EA1110-CHNS-O elemental analyzer. Fourier-transform infrared (FT-IR) spectra were recorded with a Nicolet Magna-IR 550 spectrometer, using dry KBr discs, in the range 4000–400 cm^{-1}. Photoluminescence spectra of the crystalline samples were recorded on a F-2500 FL spectrophotometer with wavelength increment 1.0 nm at room temperature using a xenon arc lamp as the excitation source. Room-temperature optical diffuse reflectance spectra of the powdered samples were obtained using a Shimadzu UV-3150 spectrometer. The absorption (α/S) data were calculated from the reflectance using the Kubelka-Munk function $\alpha/S = (1 - R)^2/2R$,[13] where R is the reflectance at a given energy, α is the absorption, and S is the scattering coefficient. Powder X-ray diffraction (PXRD) patterns were collected on a D/MAX-3C diffractometer using graphite monochromatized CuKα radiation (λ = 1.5406 Å). Thermal gravimetric analyses (TGA) were conducted on an SDT 2960 microanalyzer; the samples were heated at a rate of 5 ºC min^{-1} under a nitrogen stream of 100 mL min^{-1}.

Syntheses of 1–6

Synthesis of $[(en)_2(PbAgI_3)]_{2n}\cdot nH_2O$ (1): PbI_2 (231 mg, 0.5 mmol), AgI (117 mg, 0.5 mmol) and KI (332 mg, 2 mmol) were dispersed in 1.5 mL of en and 3 mL of N,N′-dimethylformamide (DMF) by stirring under ambient conditions. The resulting dispersion was sealed into a polytetrafluoroethylene (PTFE)-lined stainless steel autoclave of volume 10 mL and heated at 100 ºC for 4 days. After cooling to ambient temperature, pale yellow crystals of **1** were collected by filtering, washed with 2-butanone and stored under vacuum (yield based on PbI_2: 64%). Elem Anal. Calcd for $C_8H_{34}N_8OPb_2Ag_2I_6$ (**1**): calcd. C, 5.82; H, 2.08; N, 6.79. Found: C, 5.74; H, 1.86; N 6.60%. IR data (KBr, cm^{-1}): 3247(s), 3120(s), 2938(s), 2869(s), 1600(s), 1582(s), 1486(s), 1381(m), 1328(m), 1316(m), 1159(w), 1099(w), 1080(s), 1028(s), 821(w), 640(m), 514 (w),441(m), 402 (w).

Synthesis of $[(pda)_2(PbAgI_3)]_n$ (2): Yellowish crystals of **2** (61% yield based on PbI_2) was prepared with a procedure similar to that for the synthesis of **1**, except that pda was used instead of ethylenediamine. Elem. Anal. Calcd for $C_6H_{20}N_4PbAgI_3$ (**2**): C, 8.54; H, 2.39; N, 6.64. Found: C, 8.41; H, 2.31; N, 6.50%. IR data (KBr, cm^{-1}): 3308(s), 3220(s), 3122(s), 2933(s), 2874(s), 1582(s), 1510(m), 1384(m), 1329(m), 1156(w), 1114(w), 1029(s), 1000(s), 949(s), 810(w), 603(m), 574(m), 481(m), 452(m).

Synthesis of $[(tmeda)(PbAgI_3)]_n$ (3). Light-yellow crystals of **3** (68% yield based on PbI_2) was prepared with a procedure similar to that for the synthesis of **1**, except that tmeda was used instead of ethylenediamine. Elem. Anal. Calcd for $C_6H_{16}N_2PbAgI_3$ (**3**): C, 8.88; H, 1.99; N, 3.45. Found: C, 8.78; H, 1.83; N 3.32%. IR data (KBr, cm^{-1}): 3050(w),2920(w), 1662(s), 1582(m), 1510(s), 1422(s), 1338(w), 1254(w), 1139(m), 1097(m), 844(s), 772(m), 726(s), 662(m), 502(w), 422(m).

Synthesis of $[(trien)(PbAgI_3)]_n$ (4). Pale yellow crystals of **4** (72% yield based on PbI_2) was prepared with a procedure similar to that for the synthesis of **1**, except that trien was used instead of ethylenediamine. Elem. Anal. Calcd for $C_6H_{18}N_4PbAgI_3$ (**4**): C, 8.56; H, 2.15; N, 6.65. Found: C, 8.44; H, 2.20; N, 6.55%. IR data (KBr, cm^{-1}): 3447(w), 3245(m), 2847(s), 2761(s), 1582(s), 1460(s), 1381(m), 1328(m), 1155(m), 1080(m), 1029(s), 1009(s), 945(m), 841(m), 790(m), 511(w), 446(m).

Synthesis of $[(tepa)(PbAg_2I_4)]_n$ (5). Light-yellow crystals of **5** (66% yield based on PbI_2) was prepared with a procedure similar to that for the synthesis of **1**, except that tepa was used instead of ethylenediamine. Elem. Anal. Calcd for $C_8H_{23}N_5PbAg_2I_4$ (**5**): C, 8.58; H, 2.07; N, 6.25. Found: C, 8.49; H, 2.01; N, 6.12%. IR data (KBr, cm^{-1}): 3232(s), 3135(s), 2899(m), 2835(m), 2325(w), 1645(w), 1565(m), 1443(m), 1359(w), 1312(m), 1177(m), 1118(m), 1004(s), 941(s), 882(m), 818(s), 607(m), 527(m), 490(m), 422(w).

Synthesis of $[\{(dien)_3(CO_3)\}_2(Pb_6Ag_8I_{15})]_nI_n$ (6). PbI_2 (231 mg, 0.5 mmol), Ag_2CO_3 (138 mg, 0.5 mmol) and KI (332 mg, 2 mmol) were dispersed in 3 mL of DMF and 1.5 mL of dien by stirring under ambient conditions. The resulting dispersion was sealed into a PTFE-lined stainless steel autoclave of volume 10 mL and heated at 120 ºC for 4 days. After cooling to ambient temperature, colorless crystals of **6** were collected by filtering, washed with 2-butanone and stored under vacuum (54% yield based on PbI_2). The reactions with AgI or $AgNO_3$ instead of Ag_2CO_3 produced no crystals of **6** but white powders. Elemental composition of the white powder matches

the compound $Pb(dien)I_2$ according to elemental analyses. Elem. Anal. Calcd for $C_{26}H_{78}N_{18}O_6Pb_6Ag_8I_{16}$ (**6**): C, 6.41; H, 1.61; N 5.17. Found: C, 6.28; H, 1.53; N 5.04%. IR data (KBr, cm^{-1}): 3388(s), 3046(m), 1625(m), 1582(m), 1510(s), 1422(s), 1338(w), 1215(w), 1144(m), 1097(m), 983(w), 844(s), 772(w), 726(s), 642(m), 578(w), 507(m), 422(s).

X-ray Crystal Structure Determinations

All data were collected on a Rigaku Saturn CCD diffractometer using graphite-monochromated Mo-*Kα* radiation (λ = 0.71073 Å) in ω-scanning mode, to a maximum 2θ of 50.70º. An empirical absorption correction was applied to the data. The structures were solved using SHELXS-97,[14a] and refinement was performed against F^2 using SHELXL-97.[14b] All the non-hydrogen atoms were refined anisotropically. The hydrogen atoms were added geometrically and refined using a riding model. The C(4)–C(6) atoms in **2** are disordered. The occupancies of the disordered atoms are refined as 70% and 30% for C/C'. Crystallographic, experimental, and analytical data for the title compounds are listed in Table 1.

Table 1 Crystallographic and refinement of **1**–**6**

	1	**2**	**3**	**4**	**5**	**6**
Empirical Formula	$C_8H_{34}N_8OAg_2Pb_2I_6$	$C_6H_{20}N_4AgPbI_3$	$C_6H_{16}N_2AgPbI_3$	$C_6H_{18}N_4AgPbI_3$	$C_8H_{23}N_5Ag_2PbI_4$	$C_{26}H_{78}N_{18}O_6Ag_8Pb_6I_{16}$
Formula weight	1649.95	844.02	811.97	842.00	1119.84	4875.56
Crystal system	monoclinic	monoclinic	monoclinic	monoclinic	orthorhombic	trigonal
Space group	*C* 2/c (no. 15)	*C*2/c (no. 15)	$P2_1$/n (no. 14)	$P2_1$/c (no. 14)	$P2_12_12_1$ (no. 19)	$P3_1$c (no. 159)
a/ Å	23.689(4)	17.688(5)	12.1274(16)	12.280(3)	10.7925(19)	12.4185(11)
b/ Å	8.2691(12)	16.817(4)	10.2793(14)	8.194(2)	12.842(2)	12.4185(11)
c/ Å	17.134(3)	12.662(3)	12.8221(18)	16.847(4)	15.722(3)	32.218(3)
β/ º	112.922(4)	111.853(6)	91.196(4)	106.311(6)	90	90
V/ Å^3	3091.4(9)	3495.7(15)	1598.1(4)	1626.9(7)	2179.0(7)	4303.0(7)
Z	4	8	4	4	4	2
T/ K	223(2)	223(2)	223(2)	223(2)	223(2)	223(2)
Measured reflections	7450	14521	15063	8006	21337	23084
Independent reflections	2809	3191	2921	2956	3984	4462
R_{int}	0.0591	0.0537	0.0535	0.0611	0.0896	0.0686
Parameters	125	139	124	119	182	243
$R1$ [$I > 2\sigma(I)$]	0.0369	0.0372	0.0344	0.0524	0.0579	0.0358
*wR*2 (all data)	0.0808	0.1526	0.1116	0.1464	0.1212	0.0621
Goodness of fit	0.935	0.982	1.013	1.082	1.114	1.023

Results and Discussion

Syntheses.

The reaction of PbI_2, AgI and KI with 1:1:4 molar ratio in mixed en and DMF solution produced pale yellow crystals of $[\{(en)_2(PbAgI_3)\}]_{2n}\cdot nH_2O$ (**1**). The same products of **1** were obtained with Pb:Ag molar ratio varying in the range 1:2–2:1. Compounds $[(pda)_2(PbAgI_3)]_n$ (**2**), $[(tmeda)(PbAgI_3)]_n$ (**3**), $[(trien)(PbAgI_3)]_n$ (**4**), and $[(tepa)(PbAg_2I_4)]_n$ (**5**) were prepared by the same reaction using pda, tmeda, trien and tepa instead of en, respectively. The reaction in dien and DMF mixed solution gave white powders of $Pb(dien)I_2$. The reaction with Ag_2CO_3 instead of AgI afforded compound $[\{(dien)_3(CO_3)\}_2(Pb_6Ag_8I_{15})]_nI_n$ (**6**). Solvent plays an important role in the syntheses. The reactions in CH_3OH or CH_3CN solvents instead of DMF under the same conditions produced no crystalline compounds. All the ethylene polyamines are combined in the final compounds to form hybrid organic-inorganic heterometallic Pb–Ag iodometallates **1**–**6**. They all coordinate to Pb(II) ions via N-donor atoms, demonstrating that Pb(II) ion exhibits higher affinity for amino group than the Ag(I) ion. Powder X-ray diffraction (PXRD) patterns of the bulk phases of samples **1**, **3** and **6** are measured. The PXRD patterns are consistent with the simulated PXRD patterns based on single-crystal XRD data (Fig. S1–S3 in the ESI), indicating that the bulk phases of **1**, **3** and **6** are pure.

Crystal Structures of 1–4.

Compound **1** crystallizes in the monoclinic space group *C*2/c, with four formula units in the unit cell. It is constructed by two $[Pb(en)_2]^{2+}$ cations, and a Ag_2I_6 unit, as well as a H_2O molecule. The Ag^+ ion is coordinated to four iodide anions at distances in the range of 2.8077(11)–2.8871(12) Å, forming an AgI_4 tetrahedron with I–Ag–I angles in the range of 103.29(4)–116.46(3)°. Two AgI_4 tetrahedra share a common edge to form the bimeric Ag_2I_6 unit with a centrosymmetric structure (Fig. 1a). The Pb^{2+} ion is coordinated to two bidentate en ligands, forming a $[Pb(en)_2]^{2+}$ unit (Fig. 1b). The Pb–N bond lengths are in the range of 2.528(10)–2.563(9) Å (Table S1), which are consistent with those of Pb(II) complexes containing en or dien amino ligands.[15] The Ag_2I_6 unit coordinates to Pb(II) ions of different $[Pb(en)_2]^{2+}$ cations with two *trans* terminal iodine atoms as a bidentate μ-1κ^2,2κ^2 bridging ligand. Each Ag_2I_6 binds four $[Pb(en)_2]^{2+}$ units, while

each $[Pb(en)_2]^{2+}$ is coordinated by two Ag_2I_6 units (Fig. 1c). As a result, the $[Pb(en)_2]^{2+}$ and Ag_2I_6 units are interlinked to form a 2-D $[\{(en)_2(PbAgI_3)\}]_{2n}$ neutral layer (Fig. 2b). The Pb–I bond lengths are 3.5504(11) and 3.5457(11) Å, which are in the upper range of 3.0355(8)–3.637(2) Å for the Pb–I bonds observed in iodoplumbates $[Yb(DMF)_8][Pb_3I_9]$ and $[Tb(DMF)_8][Pb_3I_9]\cdot DMF$.[7,12] Besides, as shown in (Fig. 1c), the Pb^{2+} ion has two iodine neighbors (I1 and I1a) at longer distances of 3.7518(11) and 3.7602(11) Å (Table S1), which are less than the sum of the van der Waals' radii of Pb and I (4.18 Å).[16] Taking into account the secondary Pb···I bonds, the Pb^{2+} ion is in an 8-fold coordination involved in four N atoms of two chelating en and four I atoms of three Ag_2I_6 units. The PbN_4I_4 polyhedron has a square antiprismatic geometry with four N atoms forming one face, and four I atoms forming the opposite face (Fig. S10 in the ESI).

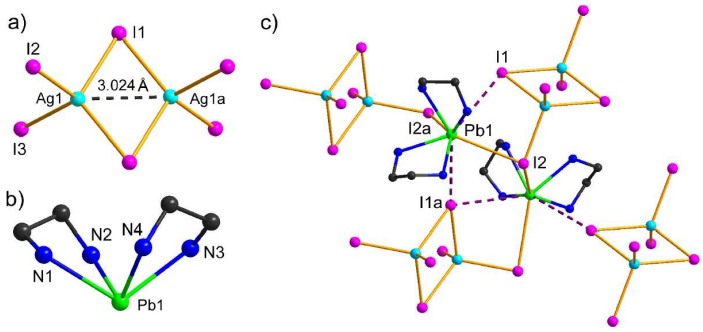

Fig. 1 Crystal structures of Ag_2I_6 (a) and $[Pb(en)_2]^{2+}$ (b) units in **1** with labeling scheme. (c) Crystal structure of **1** showing the complete coordination sphere of Pb^{2+} ion. H_2O molecule and hydrogen atoms are omitted for clarity.

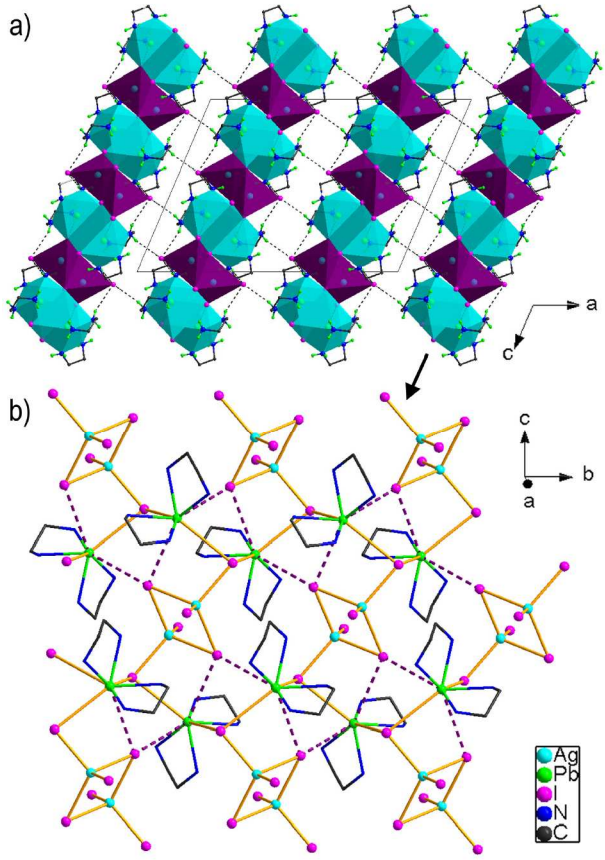

Fig. 2 (a) Polyhedral graph of **1** along the *b* axis, showing the N–H···I H-bonding in dashed line (H_2O molecule is omitted for clarity). PbN_4I_4 units are shown as green polyhedra, and AgI_4 are shown as purple tetrahedra. (b) View of the $[\{(en)_2(PbAgI_3)\}]_{2n}$ layer in **1.** Hydrogen atoms are omitted for clarity.

In the $[\{(en)_2(PbAgI_3)\}]_{2n}$ layer, each Ag_2I_6 unit is connected with six $[Pb(en)_2]^{2+}$ cations via I1 and I2 atoms (Fig. S11). The $[\{(en)_2(PbAgI_3)\}]_{2n}$ layers run parallel to (100) face of the unit cell (Fig. 2a), and the water molecules are located between the layers. The terminal I3 atom contacts with the $N(3)H_2$ group of the same layer via N–H···I hydrogen bonds (N3–HA···I3, 3.848(9) Å) (Table S7). It interacts with the $N(3)H_2$ group belonging to the neighboring layer, forming interlayer N–H···I hydrogen bond (N3–HB···I3, 3.719(9) Å) (Fig. S12 in the ESI). The interlayer N–H···I hydrogen bond connected the $[\{(en)_2(PbAgI_3)\}]_{2n}$ layers into a 3-D network structure. The N···I distances are comparable to those observed in other iodometallates.[3c,4g]

Compound **2** has similar crystal structure to **1**. It is composed of two $[Pb(pda)_2]^{2+}$ cations, and a Ag_2I_6 unit (Fig. 3). The Ag–I bond lengths vary in 2.818(3)–2.874(3) Å (Table S2). The Pb^{2+} ion is coordinated to two bidentate pda ligands, forming the complex cations $[Pb(pda)_2]^{2+}$ (Fig. 3b). The Pb–N bond lengths [2.41(2)–2.60(3) Å] (Table S2) are consistent with those in compound **1**. Acting as a bidentate μ-1κ,2κ bridging ligand, the Ag_2I_6 unit bridges two $[Pb(pda)_2]^{2+}$ cations with two *trans* terminal iodine anions (I2 and I2a) to form the neutral heterometallic Pb-Ag iodometallate $[(pda)_2(PbAgI_3)]_n$. Each $[Pb(pda)_2]^{2+}$ cation is coordinated by two Ag_2I_6 units with Pb–I bond lengths of 3.466(3) and 3.619(3) Å (Fig. 3b, Table S2). In addition, the Pb^{2+} ion has two iodine neighbors (I3 and I3a) at longer distances of 3.672(3) and 4.187(3)Å (Table S2). The Pb^{2+} ion is also in an 8-fold coordination involved in four N and four I atoms. The PbN_4I_4 polyhedron has a much distorted square antiprismatic geometry. Unlike the Ag_2I_6 unit of **1**, which binds the Pb^{2+} ions with a terminal and a bridging I atoms, the Ag_2I_6 unit of **2** coordinates the Pb^{2+} ions with two terminal I atoms (Fig. 3c). Each Ag_2I_6 unit is connected with six $[Pb(pda)_2]^{2+}$ cations via I2 and I3 atoms (Fig. 3, Fig. S13).

In the crystal structure of **2**, the $[Pb(pda)_2]^{2+}$ and Ag_2I_6 units are connected into a layer via Pb–I bonds and secondary Pb···I bonds. The layers stack parallel along the *c* axis, and are connected via interlayer Pb···I bonds forming a 3-D network, in which elliptical 1-D channel is formed (Fig. 4a). The channel is constructed by four Ag_2I_6 and eight $[Pb(pda)_2]^{2+}$ units, and all the CH_3 groups of the pda ligands are accommodated in the channels (Fig. 4b).

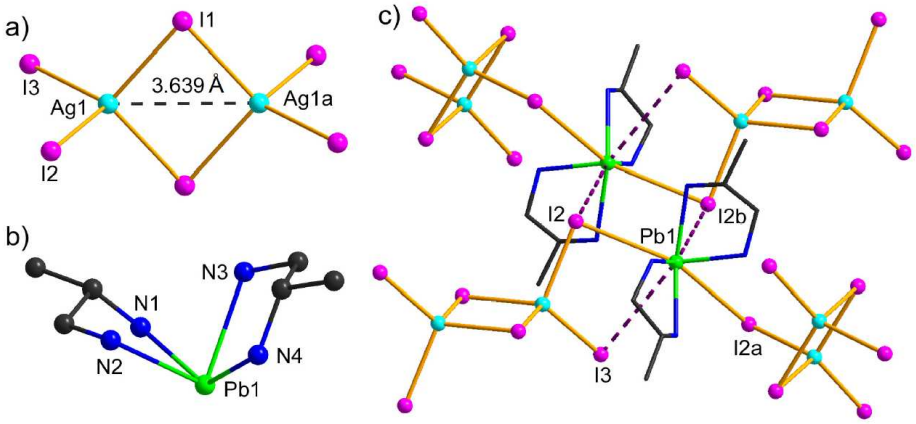

Fig. 3 Crystal structures of Ag_2I_6 (a) and $[Pb(pda)_2]^{2+}$ (b) units in **2** with labeling scheme. (c) Crystal structure of **2** showing the complete coordination sphere of Pb^{2+} ion. Hydrogen atoms are omitted for clarity.

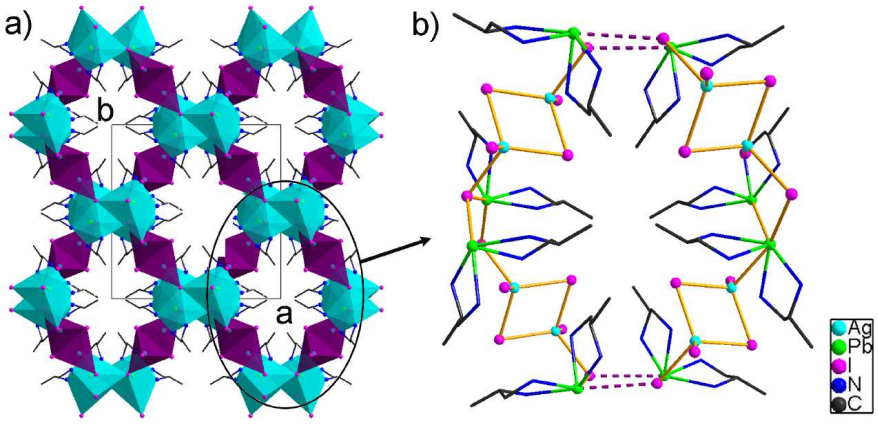

Fig. 4 (a) Polyhedral graph of **2** viewed along the *c* axis. PbN_4I_4 units are shown as green polyhedra, and AgI_4 are shown as purple tetrahedra. (b) View of the $[(pda)_2(PbAgI_3)]_n$ layer in **2.** Hydrogen atoms are omitted for clarity.

Compound **3** is composed of two $[Pb(tmeda)]^{2+}$ and a Ag_2I_6 unit (Fig. 5a and 5b). Unlike the Pb^{2+} ions in **1** and **2** which are coordinated by two bidentate en and pda ligands, the Pb^{2+} ion is coordinated to only one bidentate tmeda ligand to form the complex cation $[Pb(tmeda)]^{2+}$ (Fig. 5b) due to higher steric hindrance of the tmeda ligand. The Pb^{2+} ion is further chelated by I1 and I3 of one Ag_2I_6 unit, and by I2 and I3 of another Ag_2I_6 unit (Fig. 5c). As a result, the Pb^{2+} ion is in a six-fold coordination involved in two N and four I atoms, forming a distorted octahedral geometry. The Pb–I bond lengths vary in 3.1103(18)–3.4141(17) Å, which are in the lower range of 3.0355(8)–3.637(2) Å for the Pb–I bonds observed in iodoplumbates,[7, 12] indicating that the connections between $[Pb(tmeda)]^{2+}$ and Ag_2I_6 units are much stronger than the corresponding connections in **1** and **2**. The steric hindrance of amino ligands also has influence on the structural parameter of the Ag_2I_6 units. The Ag···Ag distance increases from 3.024 Å to 3.639 Å, and to 3.788 Å with the I1–Ag–I1a angles decreasing from 116.46(3)° to 101.28(9)°, and to 97.80(7)° for **1**–**3** (Tables S1–S3), indicating the steric hindrance of amino ligands are in the increasing order: en < pad < tmeda. It is noteworthy that there is no Pb···I secondary interactions in compound **3**.

In **3**, the Ag_2I_6 unit chelates a $[Pb(tmeda)]^{2+}$ cation with I1 and I3 atoms, and another $[Pb(tmeda)]^{2+}$ cation with I2 and I3 atoms. As a result, each Ag_2I_6 unit connects four $[Pb(tmeda)]^{2+}$ cations as a hexadentate bridging ligand (Fig. S14), leading to layered heterometallic iodometallate $[(tmeda)(PbAgI_3)]_n$. The layers stack parallel to the (101) plane of the unit cell (Fig. 6, Fig. S15). Heterometallic 12-membered $Pb_4Ag_2I_6$ rings are formed the $[(tmeda)(PbAgI_3)]_n$ layers.

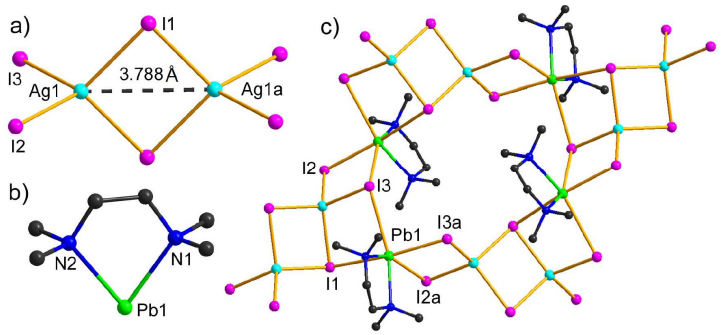

Fig. 5 Crystal structures of Ag_2I_6 (a) and $[Pb(tmeda)]^{2+}$ (b) units in **3** with labeling scheme. (c) Crystal structure of **3**.

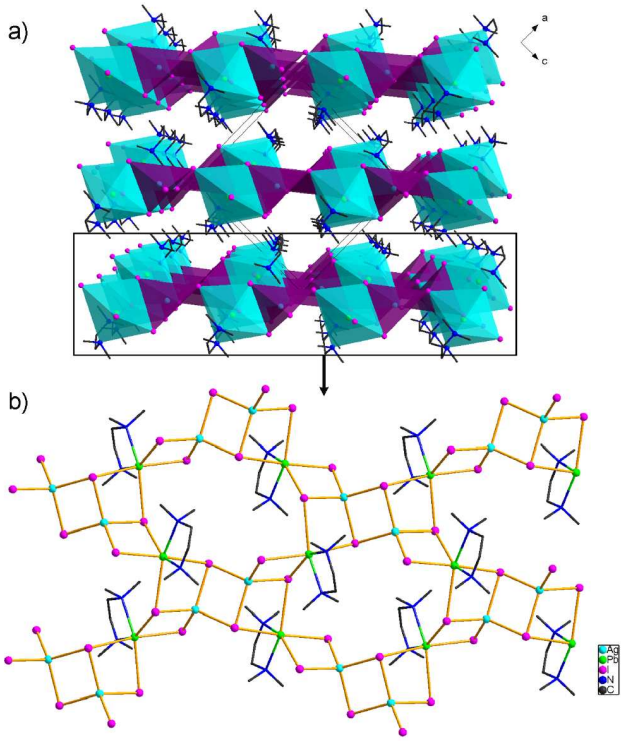

Fig. 6 (a) Polyhedral graph of **3** viewed along the *b* axis. PbN_2I_4 units are shown as blue octahedra, and AgI_4 are shown as purple tetrahedra. (b) View of the $[(tmeda)(PbAgI_3)]_n$ layer in **3.** Hydrogen atoms are omitted for clarity.

Compound **4** consists of $[Pb(trien)]^{2+}$ and Ag_2I_6 units (Fig. 7a and 7b). The Pb^{2+} ion is coordinated to a trien to form complex cation $[Pb(trien)]^{2+}$ (Fig. 7b). $[Pb(trien)]^{2+}$ and $[Pb(en)_2]^{2+}$ cations have very similar structures because a tetradentate trien corresponds to two bidentate en ligands joined by a $-CH_2CH_2-$ group (Fig. 1b, 7b). As a result, the structural parameters of $[Pb(trien)]^{2+}$ and Ag_2I_6 units are similar with corresponding values of **1** (Tables S1 and S4). The $[Pb(trien)]^{2+}$ and Ag_2I_6 units are connected via Pb–I and Pb···I bonds to form the $[(trien)(PbAgI_3)]_n$ layer parallel to the (100) face of unit cell (Fig. S16).

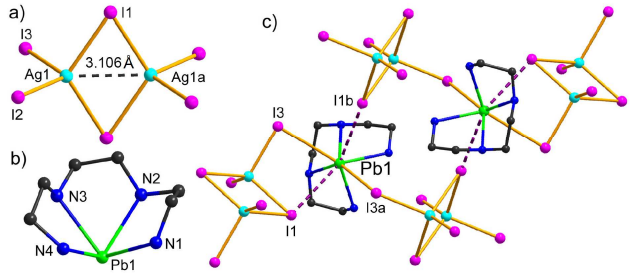

Fig. 7 Crystal structures of Ag_2I_6 (a) and $[Pb(trien)]^{2+}$ (b) units in **4** with labeling scheme. (c) Crystal structure of **4** showing the complete coordination sphere of Pb^{2+} ion. Hydrogen atoms are omitted for clarity.

Crystal Structure of 5

Compound **5** is composed of a polymeric $[Ag_2I_4]_n$ unit and $[Pb(tepa)]^{2+}$ complex cations (Fig. 8). There are two crystallographically independent Ag^+ cations, and four iodide anions. Both Ag^+ ions are coordinated by four iodide anions at distances in the range of 2.866(2)–2.884(2) Å (Table S5), which are in accordance with those of the bimeric Ag_2I_6 units in **1**–**4** (Tables S1–S4). The AgI_4 units are joined via sharing common edges to form an 1-D polymeric $[Ag_2I_4]_n^{2n-}$ anion (Fig. 8). The Ag···Ag distance of 3.137(3) Å indicates metal-matel interaction between Ag(1) and Ag(2) in the chain. The Pb^{2+} ion is coordinated by a pentadentate tepa ligand to form the complex cation $[Pb(tepa)]^{2+}$ (Fig. 8). The Pb^{2+} ion is connected to I2 of the $[Ag_2I_4]_n^{2n-}$ chain, and I4 of the neighbor $[Ag_2I_4]_n^{2n-}$ chain via Pb–I bonds. Secondary Pb···I interaction is observed between Pb1 and I1 (Fig. 8). Therefore, the Pb^{2+} ion is in an 8-fold coordination environment involved in five N and three I atoms, forming a distorted octahedral geometry. In the crystal structures of **5**, each $[Ag_2I_4]_n^{2n-}$ chain is coordinated by four arrays of $[Pb(tepa)]^{2+}$ cations via Pb–I [3.572(3), 3.6750(16) Å] and Pb···I [3.953(3) Å] bonds (Table S5). Every two $[Ag_2I_4]_n^{2n-}$ chains is joined at I1, I2, and I4 by the $[Pb(tepa)]^{2+}$ cations (Fig. S17). As a result, the $[Ag_2I_4]_n^{2n-}$ chains and $[Pb(tepa)]^{2+}$ cations are connected to form a 3-D network via Pb–I and Pb···I bonds, as well as N–H···I hydrogen bond interactions (Fig. 9, Fig. S17).

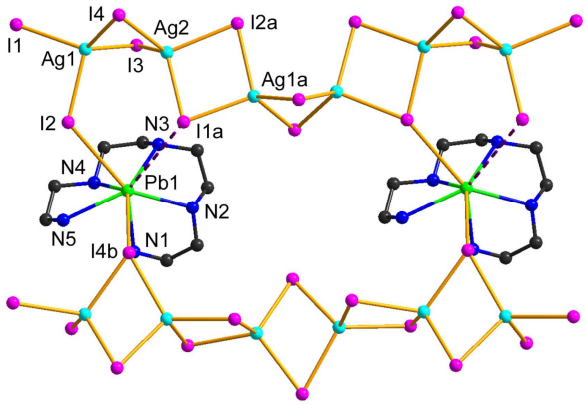

Fig. 8 Crystal structure of **5** with labeling scheme, showing the complete coordination sphere of Pb^{2+} ion. Hydrogen atoms are omitted for clarity.

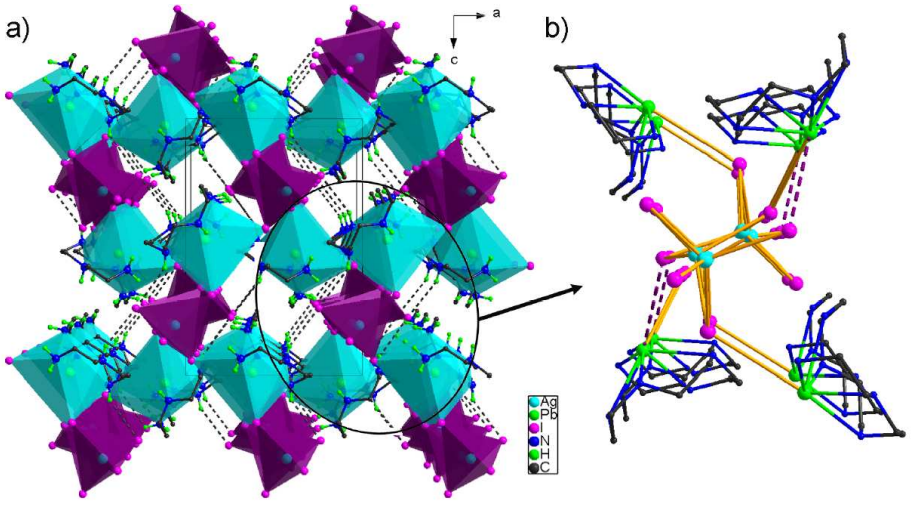

Fig. 9 (a) Polyhedral graph of **5** viewed along the *b* axis. PbN_5I_3 units are shown as blue polyhedra, and AgI_4 are shown as purple tetrahedra. (b) Coordination environment of the $[Ag_2I_4]_n^{2n-}$ chain in **5**. Hydrogen atoms are omitted for clarity.

Crystal Structure of 6

Compound **6** crystallizes in the trigonal crystal system in space group $P3_1c$. It is composed of $[\{Pb(dien)\}_3(CO_3)]^{4+}$ unit, Ag_8I_{15} cluster and a free iodide anion. There are two crystallographically independent Pb atoms in **6**. Both Pb(1) and Pb(2) are coordinated by a tridentate dien ligand, forming $[Pb(dien)]^{2+}$ units. Acting as a μ_3-CO_3 tridentate bridging ligand, the CO_3^{2-} ion binds three $[Pb(1)(dien)]^{2+}$ units to form the novel trinuclear $[\{Pb(1)(dien)\}_3(\mu_3\text{-}CO_3)]^{4+}$ complex ion (Fig. 10). Another $[\{Pb(2)(dien)\}_3(\mu_3\text{-}CO_3)]^{4+}$ ion is constructed by three $[Pb(2)(dien)]^{2+}$ units and a CO_3^{2-} ion with the same connections (Fig. S18). The Pb–N [2.533(12)–2.626(17) Å] and Pb–O [2.356(8), 2.374(9) Å] (Table S6) bond lengths are accordance with those reported.[15,17] The structural evolution of the Ag_8I_{15} cluster is depicted in Fig. 11 to elucidate its complex structure. Six AgI_4 tetrahedra are connected end to end via sharing common edges to give a cyclic Ag_6I_{13} subunit (Fig. 11a). The Ag_6I_{13} subunit is capped by Ag(3)I at the face of I3, I3a and I3b, and by Ag(4)I at the face of I5, I5a and I5b, to form the Ag_8I_{15} cluster in C_3 symmetry (Fig. 11b). In other word, the Ag_8I_{15} cluster is constructed by eight AgI_4 tetrahedra via edge- and face-sharing. Ag3, Ag4, I1, I6 and I7 five atoms are in the same line, which is just the C_3 axis of the Ag_8I_{15} cluster. In the Ag_8I_{15} cluster, the central iodide anion (I1) coordinates to six Ag(I) ions as a μ_6-I ligand (Fig. 11a). Except for I1 as a μ_6-I coordination mode, the rest iodide anions adopt doubly bridging (I2, I3, I4, I5) or terminal (I6, I7) coordination modes. Correspondingly, the Ag–I bond lengths increase in the order: Ag–I [av.: 2.767(4) Å] < Ag–μ-I [av.: 2.8226(18) Å] < Ag–μ_6-I [av.: 2.9782(18) Å]. The bond length of Ag–μ_6-I is shorter than those of Ag–μ_9-I [3.059(3)–3.317(2) Å] and Ag–μ_{12}-I [3.380(1) Å] observed in polyneclear iodoargentates.[10b, 10c]

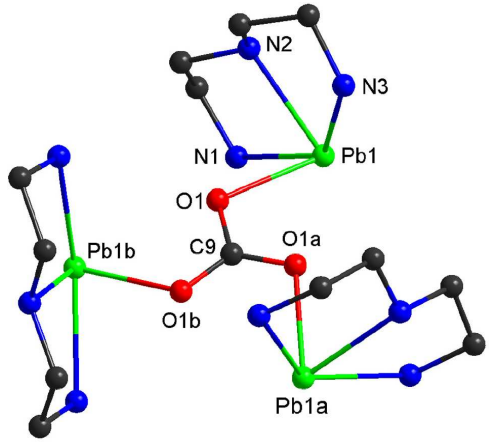

Fig. 10 Crystal structure of the $[\{Pb(1)(dien)\}_3(\mu_3\text{-}CO_3)]^{4+}$ unit in **6** with labeling scheme.

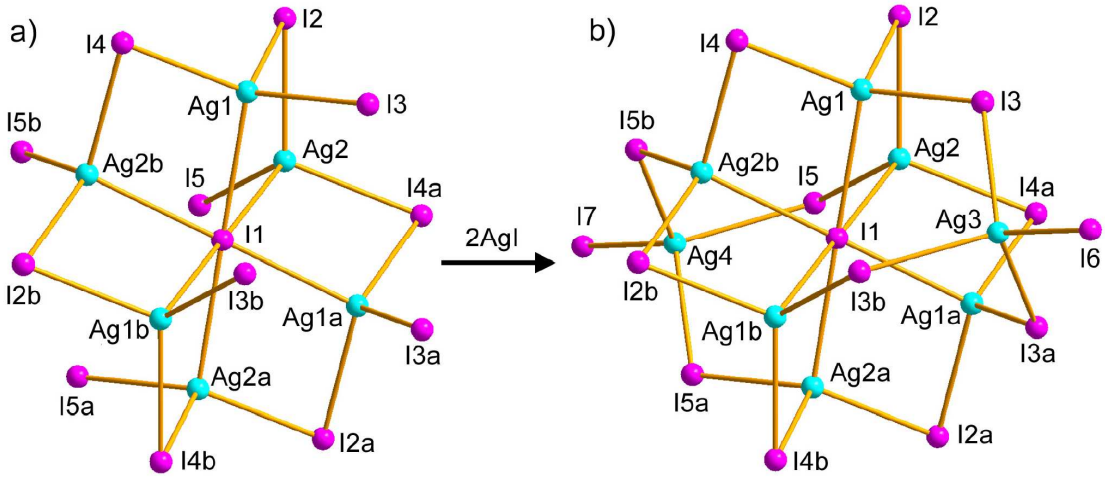

Fig. 11 Structural evolution of the Ag_8I_{15} cluster in **6**, showing crystal structure of the Ag_6I_{13} subunit (a), and Ag_8I_{15} cluster (b).

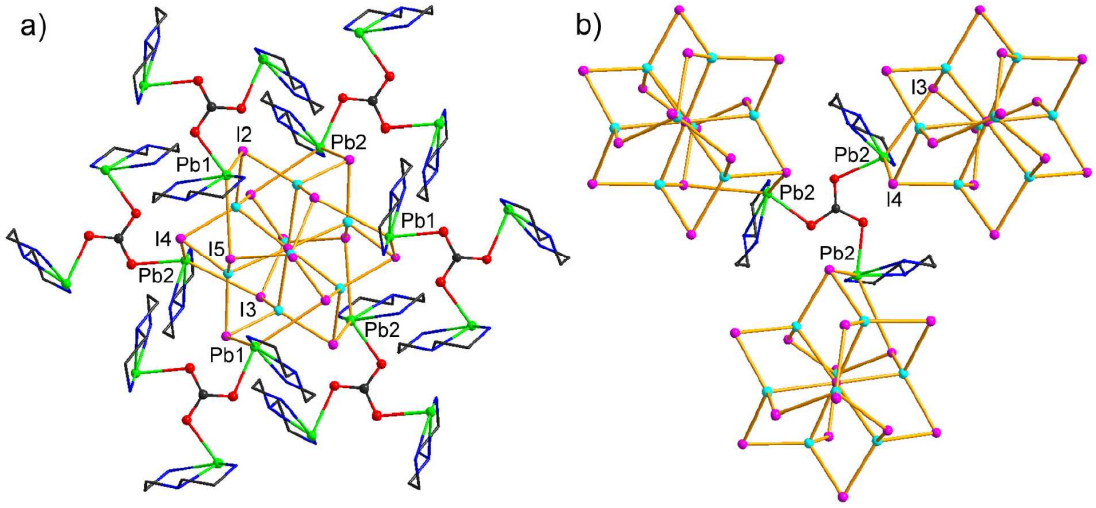

Fig. 12 Structure environments of the Ag_8I_{15} cluster (a) and $[\{Pb(2)(dien)\}_3(CO_3)]^{4+}$ unit (b) in **6**.

The Ag_8I_{15} cluster is connected with $[\{Pb(dien)\}_3(CO_3)]^{4+}$ unit via Pb–I bonds. It binds the Pb^{2+} ion of $[\{Pb(1)(dien)\}_3(CO_3)]^{4+}$ with I2 and I5, and the Pb^{2+} ion of $[\{Pb(2)(dien)\}_3(CO_3)]^{4+}$ with I3 and I4 (Fig. 12a). The Pb–I bond lengths are in the range of 3.5784(14)–3.6311(11) Å (Table S6), which are in accordance with those observed in **1**, **2**, **4**, and **5**. Both Pb(1) and Pb(2) are in 6-fold coordination environments involved in three N, two I, and one O atoms, forming much distorted octahedral geometries. Each Ag_8I_{15} cluster is surrounded by three $[\{Pb(1)(dien)\}_3(CO_3)]^{4+}$ and three $[\{Pb(2)(dien)\}_3(CO_3)]^{4+}$ units (Fig. 12a), while each $[\{Pb(dien)\}_3(CO_3)]^{4+}$ unit binds three Ag_8I_{15} clusters (Fig. 12b). As a result, the Ag_8I_{15} clusters and $[\{Pb(dien)\}_3(CO_3)]^{4+}$ units are joined to form a layered cation $[\{(dien)_3(CO_3)\}_2(Pb_6Ag_8I_{15})]_n^{n+}$ (Fig. S19). The cationic $[\{(dien)_3(CO_3)\}_2(Pb_6Ag_8I_{15})]_n^{n+}$ layers are perpendicular to *c* axis of the unit cell, and the free I^- ion is located between the layers. The interlayered N–H···I hydrogen bonds connect the layers into a 3-D network.

Optical absorption and photoluminescent properties

Solid-state optical absorption spectra of powder samples of **1**–**6**, and PbI_2 and AgI solids were measured at room temperature. The absorption data calculated from the reflectance spectra using the Kubelka–Munk function[12] demonstrate that compounds **1**–**6** show well-defined abrupt absorption edges from which the band gaps can be estimated as 2.87, 2.85, 2.71, 2.88, 2.80, and 3.20 eV, respectively (Fig. 13), indicating that the present compounds are potential semiconductors. They have 0.40–0.89 eV blue shift of the absorption edges compared with those of the bulk PbI_2 (2.31 eV) and AgI (zinc-blend structure, ~2.40 eV)[18] solids (Fig. 14). This observation is accordance with the "dimensional reduction" (DR) effect caused by the polyamines in compounds **1**–**6**. DR dismantles a dense three-dimensional (3-D) structure to a lower-dimensional network by the electronegative molecules of polyamines, which results in an increase of the energy band gap.[19]

The photoluminescent properties of all samples were measured at room temperature. An intense PL emission was observed for compounds **5** and **6** upon photoexcitation at 280 nm (Fig. 14). Compound **5** exhibits a photoluminescent emisson band at 518 nm. Compound **6** gives a photoluminescent emisson at 539 nm, and a weak shoulder peak at 582 nm. The emission bands are higher than that of the Ph_3P-hybrid tetrameric silver iodide $(Ph_3P)_4Ag_4I_4$, whose photoluminescent emisson occurs at 418 or 455 nm.[10a] Compounds **1**–**4** are PL-inactive.

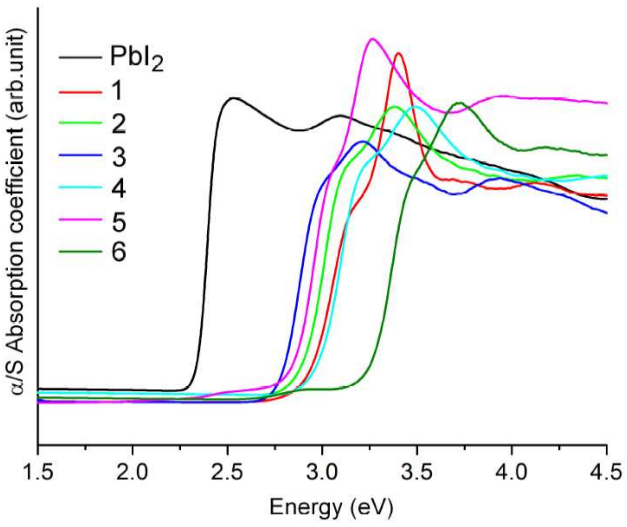

Fig. 13 Optical absorption spectra of compounds **1**–**6**, and PbI_2.

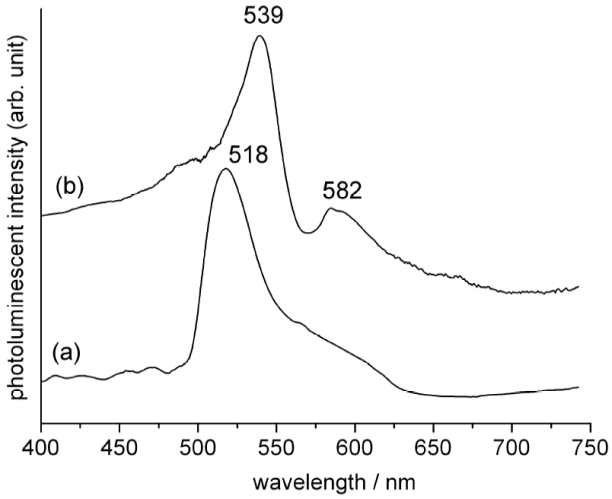

Fig. 14 Photoluminescent spectra of compounds **5** (a) and **6** (b) at room temperature. The photoluminescent spectra were excited by 280 nm light from a xenon arc lamp.

Thermal properties

The thermal stabilities of compounds **1**, **4**, and **5** were investigated using TG-DTA method under a nitrogen atmosphere in the range of 25–450°C. Compound **1** shows a two-step thermal decomposition process (Fig. S20). It decomposes at T_{onset} = 190 ºC with total mass losses of 12.1% before 450 ºC. The total mass loss is in accordance with the removal of its all en ligands and H_2O molecule (theoretical values: 13.4%). The decomposition is accompanied by strong endothermic signals in the DTA curve with the peak temperatures 211ºC and 272 ºC. Compounds **4** and **5** lose their amino ligands in one step between 220ºC and 450 ºC with mass losses of 16.8% and 16.7%, respectively. The observed mass losses are in accordance with the theoretical value for the complete removal of trien and tepa ligands (theoretical values: 17.4% for **4**, 17.7% for **5**). The loss of organic ligands are accompanied by one endothermic signal in the DTA curves, with peak temperatures at 293 °C for **4**, and 334 °C for **5** (Fig. S19). These observations demonstrate that thermal stabilities increase in the order: **1**< **4** < **5**, indicating chelating effects increase from en to trien to tepa.

Conclusions

In summary, the solvothermal reactions of PbI_2, AgI (or Ag_2CO_3) and KI with different ethylene polyamines in DMF afforded a series of Pb-Ag heterometallic iodides, **1**–**6**, decorated by polyamine at Pb(II) ions via Pb–N bonds. These heterometallic iodides contain backbones of 2-D layers of $[PbAgI_3]_n$ (**1**, **3**, **4**) and $[(\mu_3\text{-}CO_3)_2(Pb_6Ag_8I_{15})]_n$ (**6**), and 3-D networks of $[PbAgI_3]_n$ (**2**) and $[PbAg_2I_4]_n$ (**5**), which are constructed by coordination of iodoargentate aggregates to the Pb^{2+} ions via iodide anions. The coordination modes and connection strength between iodoargentate aggregates and the Pb^{2+} ions are influenced by the steric hindrance and denticity of ethylene polyamines. Title compounds remove coordinated organic components between 272–334 °C, indicating good thermal stability of the organic hybrid Pb-Ag iodometallates. Compounds **1**–**6** show 0.40–0.89 eV blue shift of the absorption edges compared with those of the bulk PbI_2 and AgI.

Acknowledgements

This work was supported by the National Natural Science Foundation of P. R. China (Nos. 21171123), the Priority Academic Program Development (PAPD) of Jiangsu Higher Education Institutions, and the Key Laboratory of Organic Synthesis of Jiangsu Province, Soochow University.

Notes and references

[a]*Key Laboratory of Organic Synthesis of Jiangsu Province, College of Chemistry, Chemical Engineering and Materials Science, Dushu Lake Campus, Soochow University, Suzhou 215123, People's Republic of China. Fax/Tel: + 86-512-65880089; E-mail: jiadingxian@suda.edu.cn*

† Electronic Supplementary Information (ESI) available: selected bond lengths and angles for **1**–**6** (Tables S1–S7), PXRD spectra (Fig.s S1–S3), IR spectra (Fig.s S4–S9), structural figures (Fig.s S10–S19), and TG-DTA curves (Fig. S20). CCDC reference numbers 975566–975571 for **1**–**6**. Crystallographic data in CIF. See DOI: 10.1039/b000000x/

1 (*a*) G. C. Papavassiliou, *Prog. Solid State Chem.*, 1997, **25**, 125–270; (*b*) R. Pardo, M. Zayat and D. Levy, *Chem. Soc. Rev.*, 2011, **40**, 672–687; (*c*) V. Laget, C. Hornick, P. Rabu, M. Drillon and R. Ziessel, *Coord. Chem. Rev.,* 1998, **178–180**, 1533–1553; (*d*) N. Mercier, N. Louvain and W. Bi, *CrystEngCom*, 2009, **11**, 720–734; (*e*) L. M. Wu, X. T. Wu and L. Chen, *Coord. Chem. Rev.*, 2009, **253**, 2787–2804.

2 (*a*) D. B. Mitzi, C. A. Feild, W. T. A. Harrison and A. M. Guloy, *Nature*, 1994, **369**, 467–469; (*b*) D. B. Mitzi, S. Wang, C. A. Feild, C. A. Chess and A. M. Guloy, *Science*, 1995, **267**, 1473–1476; (*c*) C. R. Kagan, D. B. Mitzi, C. D. Dimitrakopoulos, *Science*, 1999, **286**, 945–947; (*d*) G. C. Papavassiliou, *Prog. Solid State Chem.*, 1997, **25**, 125–270; (*e*) C. H. Arnby, S. Jagner and I. Dance, *CrystEngComm.*, 2004, **6**, 257–275; (*f*) J. L. Knutson, J. D. Martin and D. B. Mitzi, *Inorg. Chem.*, 2005, **44**, 4699–4705; (*g*) A. Kojima, K. Teshima, Y. Shirai and T. Miyasaka, *J. Am. Chem. Soc.,* 2009, **131**, 6050–6051.

3 (*a*) S. Wang, D. B. Mitzi, C. A. Feild and A. M. Guloy, *J. Am. Chem. Soc.*, 1995, **117**, 5297–5302; (*b*) D. B. Mitzi, *Chem. Mater.*, 1996, **8**, 791–800; (*c*) N. Mercier, S. Poiroux, A. Riou and P. Batail, *Inorg. Chem.,* 2004, **43**, 8361–8366; (*d*) N. Mercier, A. L. Barres, M. Giffard, I. Rau, F. Kajzar and B. Sahraoui, *Angew. Chem. Int. Ed.* **2006**, *45*, 2100–2103; (*e*) S. Sourisseau, N. Louvain, W. Bi, N. Mercier, D. Rondeau, F. Boucher, J.-Y. Buzaré and C. Legein, *Chem. Mater.*, 2007, **19**, 600–607; (*f*) C. C. Stoumpos, C. D. Malliakas and M. G. Kanatzidis, *Inorg. Chem.*, 2013, **52**, 9019–9038; (*g*) T. Baikie, Y. Fang, J. M. Kadro, M. Schreyer, F. Wei, S. G. Mhaisalkar, M. Graetzel and T. J. White, *J. Mater. Chem. A*, 2013, **1**, 5628–5641.

4 (*a*) H. Krautscheid and F. Vielsack, *Angew. Chem. Int. Ed.*, 1995, **34**, 2035–2037; (*b*) H. Krautscheid and F. Vielsack, *J. Chem. Soc., Dalton Trans.*, 1999, 2731–2735; (*c*) H. Krautscheid and F. Vielsack, *Z. Anorg. Allg. Chem.*, 2000, **626**, 3–5; (*d*) H. Krautscheid, C. Lode, F. Vielsack and H. Vollmer, *J. Chem. Soc., Dalton Trans.*, 2001, 1099–1104; (*e*) V. Chakravarthy and A. M. Guloy, *Chem. Commun.*, 1997, 697–698; (*f*) Z. Tang and A. M. Guloy, *J. Am. Chem. Soc.*, 1999, **121**, 452–453; (*g*) N. Louvain, W. Bi, N. Mercier, J.-Y. Buzaré, C. Legein and G. Corbel, *Dalton Trans.*, 2007, 965–970; (*h*) D. B. Mitzi, *Prog. Inorg. Chem.*, 1999, **48**, 1–121; (*i*) D. G. Billing and A. Lemmerer, *CrystEngComm*, 2007, **9**, 236–244; (*j*) H. Krautscheid and F. Vielsack, *Z. Anorg. Allg. Chem.*, 1997, **623**, 259–263; (*k*) H. Krautscheid, F. Vielsack and N. Klaassen, *Z. Anorg. Allg. Chem.*, 1998, **624**, 807–812; (*l*) Z. J. Zhang, G. C. Guo, G. Xu, M. L. Fu, J. P. Zou and J. S. Huang, *Inorg.Chem.*, 2006, **45**, 10028–10030; (*m*) Z. J. Zhang, S. C. Xiang, G. C. Guo, G. Xu, M. S. Wang, J. P.

Zou, S. P. Guo and J. S. Huang, *Angew. Chem. Int. Ed.*, 2008, **47**, 4149–4152.

5 (*a*) S. Olson, G. Helgesson and S. Jagner, *Inorg. Chim. Acta.*, 1994, **217**, 15–20; (*b*) H. H. Li, Z. R. Chen, C. C. Huang, Y. G. Ren and Q. H. Chen, *Chin. J. Struct. Chem.*, 2004, **23**, 288−291; (*c*) H. H. Li, Z. R. Chen, C. C. Huang, Y. G. Ren and G. C. Xiao, *Chin. J. Struct. Chem.*, 2004, **23**, 1009−1012; (*d*) H. H. Li, Z. R. Chen, J. Q. Li, C. C. Huang, Y. F. Zhang and G. X. Jia, *Cryst. Growth Des.*, 2006, **6**, 1813−1820; (*e*) N. Kuhn, Q. Abu-Salem, C. Maichle-Mößmer and H. Schubert, *Z. Kristallogr. NCS.*, 2008, **223**, 341–342.

6 (*a*) Z. J. Zhang, S. C. Xiang, Y. F. Zhang, A. Q. Wu, L. Z. Cai, G. C. Guo and J.-S. Huang, *Inorg. Chem.*, 2006, **45**, 1972–1977; (*b*) J. P. Li, L. H. Li, L. M. Wu and L. Chen, *Inorg. Chem.*, 2009, **48**, 1260–1262; (*c*) M. A. Tershansy, A. M. Goforth, L. Peterson, M. C. Burns, M. D. Smith and H. -C. zur Loye, *Solid State Sci.* 2007, **9**, 895–906.

7 (*a*) S. Mishra, E. Jeanneau, S. Daniele, G. Ledoux and P. N. Swamy, *Inorg. Chem.*, 2008, **47**, 9333–9343; (*b*) S. Mishra, E. Jeanneau, O. Iasco, G. Ledoux, D. Luneau and S. Daniele, *Eur. J. Inorg. Chem.*, 2012, 2749–2758.

8 (*a*) L. G. Li, H. H. Li, Z. R. Chen, C. C. Huang, B. Zhao and J. Q. Li, *Chin. J. Struct. Chem.*, 2006, **25**, 149−152; (*b*) Y. S. Jiang, H. G. Yao, S. H. Ji, M. Ji and Y. L. An, *Inorg. Chem.*, 2008, **47**, 3922–3924; (*c*) H. H. Li, Z. R. Chen, L. G. Sun, Z. X. Lian, X. B. Chen, J. B. Li and J. Q. Li, *Cryst. Growth Des.*, 2010, **10**, 1068−1073.

9 (*a*) S. Mishra, E. Jeanneau, S. Daniele and G. Ledoux, *Dalton Trans.*, 2008, 6296−6304; (*b*) S. Mishra, E. Jeanneau, G. Ledoux and S. Daniele, *Dalton Trans.*, 2009, 4954–4961.

10 (*a*) M. Henary and J. I. Zink, *Inorg. Chem.,* 1991, **30**, 3111−3112; (*b*) Y.-J. Li, C. Latouche, S. Kahlal, J.-H Liao, R. S. Dhayal, J.-Y. Saillard and C. W. Liu, *Inorg. Chem.*, 2012, **51**, 7439−7441; (c) J.-H Liao, C. Latouche, B. Li, S. Kahlal, R. J.-Y. Saillard and C. W. Liu, *Inorg. Chem.,* 2014, **53**, 2260–2267.

11 (*a*) C. Feldmann, *Inorg. Chem.*, 2001, **40**, 818–819; (*b*) L. Q. Fan, L. M. Wu and L. Chen, *Inorg. Chem.*, 2006, **45**, 3149–3151; (*c*) W. X. Chai, L. M. Wu, L. Q. Li and L. Chen, *Inorg. Chem.*, 2007, **46**, 1042–1044; (*d*) W. X. Chai, L. M. Wu, L. Q. Li and L. Chen, *Inorg. Chem.*, 2007, **46**, 8698–8704; (*e*) M. W. Yuan, L. H. Li and L. Chen, *Z. Anorg. Allg. Chem.*, 2009, **635**, 1645–1649.

12 F. Wang, C. Y. Tang, R. H. Chen, D. X. Jia, W. Q. Jiang and Y. Zhang, *Dalton Trans.*, 2013, **42**, 15150–15158.

13 W. W. Wendlandt and H. G. Hecht, Reflectance Spectroscopy; InterscicencePublishers:New York, 1966.

14 (*a*) G. M. Sheldrick, *SHELXS-97, Program for Crystal Structure Determination*; University of Göttingen: Germany, 1997; (*b*) G. M. Sheldrick, *SHELXL-97, Program for the Refinement of Crystal Structures*; University of Göttingen: Germany, 1997.

15 (*a*) D. L. Turner, T. P. Vaid, P. W. Stephens, K. H. Stone, A. G. DiPasquale and A. L. Rheingold, *J. Am. Chem. Soc.*, 2008, **130**, 14–15; (*b*) D. L. Turner, K. H. Stone, P. W. Stephens, A. Walsh, M. P. Singh and T. P. Vaid, *Inorg. Chem.*, 2012, **51**, 370–376.

16 A. Bondi, *J. Phys. Chem.*, *B.* 1964, **68**, 441–451.

17 (*a*) Y. Li, S. V. Krivovichev and P. C. Burns, *J. Solid State Chem.*, 2000, **153**, 365–370; (*b*) C. Gabriel, C. P. Raptopoulou, V. Psycharis, A. Terzis, M. Zervou, C. Mateescu and A. Salifoglou, *Cryst. Growth Des*., 2011, **11**, 382–395.

18 (*a*) R. H. Victora, *Phys. Rev. B* 1997, *56*, 4417–4421; (*b*) D. B. Pedersen, S. Wang, *J. Phys. Chem. C* 2007, *111,* 1261–1267.

19 (*a*) T. J. McCarthy and M. G. Kanatzidis, *Inorg. Chem.*, 1995, **34**, 1257–1267; (*b*) C. Rumpf, R. Tillinski, C. Nather, P. Durichen, I. Jess and W. Bensch, *Eur. J. Solid State Inorg. Chem.*, 1997, **34**, 1187–1198; (*c*) E. A. Axtell, Y. Park, K. Chondroudis and M. G. Kanatzidis, *J. Am. Chem. Soc.*, 1998, **120**, 124–136; (*d*) C. R. Evenson and P. K. Dorhout, *Inorg. Chem.*, 2001, **40**, 2884–2891; (*e*) E. G. Tulsky and J. R. Long, *Chem. Mater.*, 2001, **13**, 1149–1166; (*f*) S. Johnsen, S. C. Peter, S. L. Nguyen, J.-H. Song, H. Jin, A. J. Freeman and M. G. Kanatzidis, *Chem. Mater.*, 2011, **23**, 4373–4383.